

Fuel-Driven Dynamic Combinatorial Libraries

Christine M. E. Kriebisch, Alexander M. Bergmann, and Job Boekhoven*



Cite This: *J. Am. Chem. Soc.* 2021, 143, 7719–7725



Read Online

ACCESS |



Metrics & More

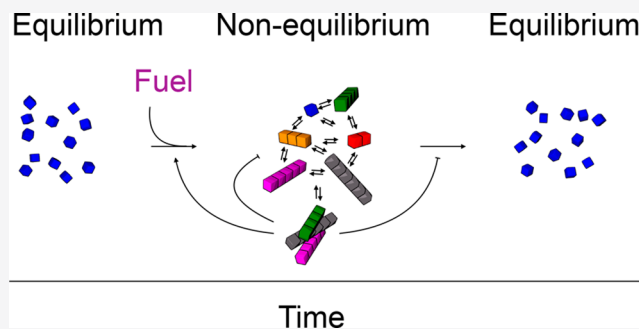


Article Recommendations



Supporting Information

ABSTRACT: In dynamic combinatorial libraries, molecules react with each other reversibly to form intricate networks under thermodynamic control. In biological systems, chemical reaction networks operate under kinetic control by the transduction of chemical energy. We thus introduced the notion of energy transduction, via chemical reaction cycles, to a dynamic combinatorial library. In the library, monomers can be oligomerized, oligomers can be deoligomerized, and oligomers can recombine. Interestingly, we found that the dynamics of the library's components were dominated by transacylation, which is an equilibrium reaction. In contrast, the library's dynamics were dictated by fuel-driven activation, which is a nonequilibrium reaction. Finally, we found that self-assembly can play a large role in affecting the reaction's kinetics via feedback mechanisms. The interplay of the simultaneously operating reactions and feedback mechanisms can result in hysteresis effects in which the outcome of the competition for fuel depends on events that occurred in the past. In future work, we envision diversifying the library by modifying building blocks with catalytically active motifs and information-containing monomers.



INTRODUCTION

In dynamic combinatorial libraries, molecules react with each other reversibly under thermodynamic control.^{1,2} The resulting library of dynamic interconverting building blocks can give rise to exciting collective behavior, like the selection of molecules that can replicate or even evolve within molecular reaction networks.^{1,2} Understanding the rudimentary behavior of such libraries is relevant to better understanding biology, which also constitutes, at the most rudimentary levels, chemical reaction networks.³ However, dynamic combinatorial libraries so far have mostly focused on libraries under thermodynamic control.^{1,2} In contrast, living systems are dissipative structures that are sustained by the constant transduction of energy via nonequilibrium chemical reactions.^{4–6} Therefore, reaction networks of living systems are partly under dynamic kinetic control.^{5,6} Models of the dynamic combinatorial chemistry in living systems that are driven by the transduction of chemical energy can increase our understanding of the role of equilibrium and nonequilibrium reactions in biological systems or at the origin of life (e.g., for RNA),⁷ which so far has been studied mostly in or close to equilibrium.^{8–10} Indeed, studies on out-of-equilibrium reaction networks in continuously stirred tank reactors result in exciting behavior like oscillations and bistability.^{11–13}

Inspired by the kinetic control in biological structure formation, synthetic analogues of such systems have been developed. In these so-called chemically fueled assemblies, energy-transducing chemical reaction cycles are regulating the activation and deactivation of molecules for self-assembly.^{14–26}

Moreover, several reaction cycles have been introduced that lead to the formulation of preliminary design rules for such structures under kinetic control.^{27–29} Despite these developments,^{27–29} only a few examples exist in which multiple building blocks compete in a transient dynamic combinatorial library.^{24,30,31} In such experiments, we may expect components of thermodynamic and kinetic control that determine the composition of the library. However, the interplay of kinetic and thermodynamic control within dynamic combinatorial libraries has not been demonstrated.

In this work, we used a well-understood chemically fueled reaction cycle¹⁴ to drive oligomerization and deoligomerization of building blocks, which are part of a dynamic combinatorial library. The oligomerization (or activation) reaction creates transient bonds between the library's components at the expense of a chemical fuel, whereas the deoligomerization (deactivation) reaction destroys these bonds spontaneously. A reversible equilibrium reaction scrambles the oligomers, resulting in a dynamic combinatorial library under kinetic control that results in recombination (Figure 1A). Excitingly, we find that assembly drastically alters the distribution of the oligomers in the library.

Received: February 9, 2021

Published: May 12, 2021



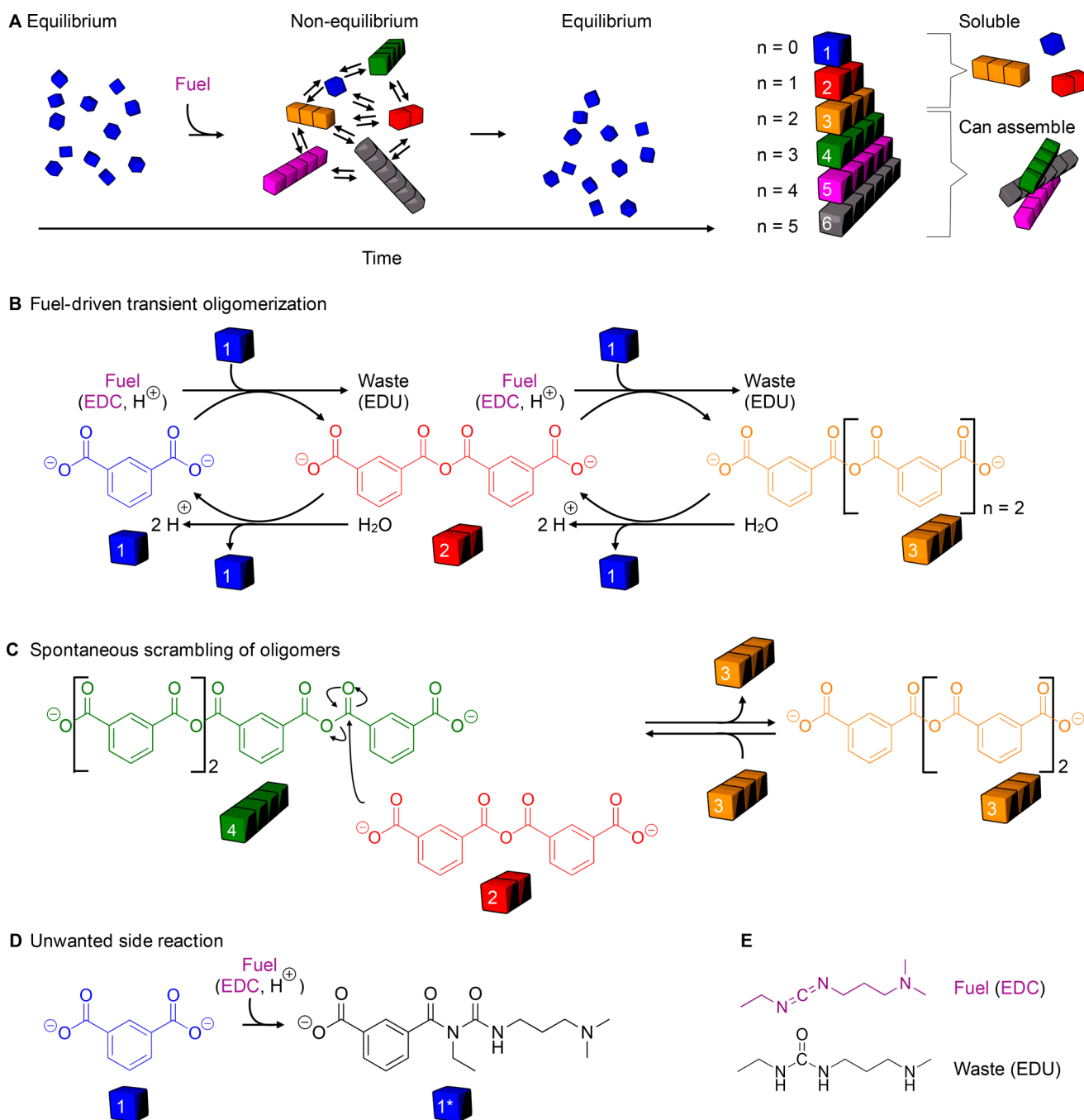


Figure 1. Description of the chemically fueled reaction network. (A) Schematic representation of the concept of a transient dynamic combinatorial library and all oligomers of the transient library. The increase in hydrophobicity decreases the solubility, making oligomers 4–6 more likely to assemble. (B) Chemical reaction network that converts a chemical fuel (EDC) into waste (EDU) while building up a transient dynamic combinatorial library. (C) Reversible equilibrium reaction, transacylation, that recombines the oligomers of the library. (D) Formation of the unwanted side product *N*-acylisourea **1***. (E) Molecular structures of fuel (EDC) and waste (EDU).

RESULTS AND DISCUSSION

We chose isophthalic acid (**1**) as a building block because it carries two carboxylates under the used conditions (500 mM MES-buffered water at pH 6) and can thus be converted into a polyanhydride. Indeed, oligomerization of isophthalic acid to polyanhydrides has been demonstrated.^{32,33} In our chemically fueled reaction cycle, two of these building blocks are condensed into their corresponding anhydride (**2**) at the expense of a condensing agent (EDC, 1-ethyl-3-(3-(dimethylamino)propyl)carbodiimide, **Figure 1E**). The prod-

uct is a dimer of the building block (**2**) and also carries two carboxylates. This dimer also can be activated and react with another monomer to yield a trimer (**3**), which can react further (**4...n**, respectively, **Figures 1B** and **S1**). Alternatively, these oligomers can be activated and react with other oligomers. In both cases, EDC-driven oligomerization increases the average length of the oligomer in the systems. In contrast, the oligomeric components in the library are prone to deoligomerize via hydrolysis. Dimer **2** can be hydrolyzed to yield two molecules of the original **1**, whereas longer oligomers can be deactivated into shorter oligomers, e.g., **4** can be hydrolyzed to

yield two molecules of **2**. In all cases, deoligomerization via hydrolysis leads to a decrease in the average oligomer length. Finally, oligomers can transacylate, i.e., an anhydride is attacked by a carboxylate of a monomer or another oligomer to yield a new anhydride and carboxylate. For example, oligomer **3** can be attacked by a monomer to yield two dimers **2**. Or, dimer **2** can attack **4**, yielding two trimers **3**, which is referred to as transacylation (Figure 1C).^{24,34,35} Transacylation scrambles the oligomers but does not change the average length of the library. We confirmed the presence of transacylation experimentally (Supporting Notes, Figure S2, and Table S1). Clearly, our chemically fueled library products are governed by the kinetics of activation, deactivation, and transacylation. Moreover, as the oligomer size increases, the oligomer becomes increasingly more hydrophobic, and we find that tetramers or higher can assemble (vide infra). Ultimately, however, the system's equilibrium state is the monomeric isophthalic acid **1**, i.e., if all fuel is depleted or no fuel is added, the system reverts to monomers. It is noteworthy that an unwanted side product, *N*-acylisourea, can be formed by the rearrangement of the activated intermediate, *O*-acylisourea (Figures 1D and S1).

We dissolved 300 mM **1** in 500 mM MES-buffered water at pH 6 with 40 mM pyridine, which are also the reaction conditions for all further experiments. We added a batch of 50 mM EDC and analyzed the emergence and evolution of the library composition and the fuel by high-performance liquid chromatography (HPLC) and mass spectrometry (Figure 2A and Tables S3 and S4). Under the applied conditions, the pH remained stable between pH 6.0 and 6.2 (Figure S3A). With a much higher concentration of EDC (i.e., >150 mM), the pH tended to noticeably increase as the cycle progressed. We found that the fuel rapidly decayed and was fully consumed after 16 min (Figure S4A), which resulted in five detectable anhydride products (**2**–**6**, Figure 2A). The major component was anhydride **2**. In contrast, **3** had a roughly 23-fold lower yield at 1 mM (Figure 2B). The concentrations of **4**, **5**, and **6** decreased further at 0.17, 0.02, and 0.0025 mM, respectively. The exponential decay of the concentration as a function of oligomer length is because the product of one reaction is the precursor for the next, e.g., **2** is required for the formation of **3**, which is required to form **4**. We followed the further evolution of the cycle. The concentrations of anhydrides **2**–**6** initially rose and then collapsed (Figures 2C and S4B–E). It is noteworthy that, as the cycle progressed, we found the emergence of an unwanted side product, i.e., the *N*-acylisourea **1*** of monomer **1**. Its concentration was <2.5 mM after the cycle was completed (Figures S4G and S1). The high concentration of precursor (300 mM) ensures that, despite the formation of **1***, a sufficient amount of **1** always is present. Indeed, experiments with only 25 or 100 mM **1** yielded a loss of 24% of **1** due to its conversion into *N*-acylisourea **1*** (Figure S3B). It is worth noting that, under these conditions, only minimal amounts of the anhydrides formed hydrolyze during the HPLC analysis (Figure S3C).

To quantitatively understand the kinetics that dominates the evolution of the library, we wrote a kinetic model that predicts the concentrations of fuel, **1**, and anhydrides **2**–**6** in response to the fuel (see the Supporting Information). The model also predicts the concentration of *N*-acylisourea **1***. The kinetic model considers the EDC-driven activation, anhydride hydrolysis, and also transacylation between the oligomers. We first fitted the EDC decay profile of the experiments to give

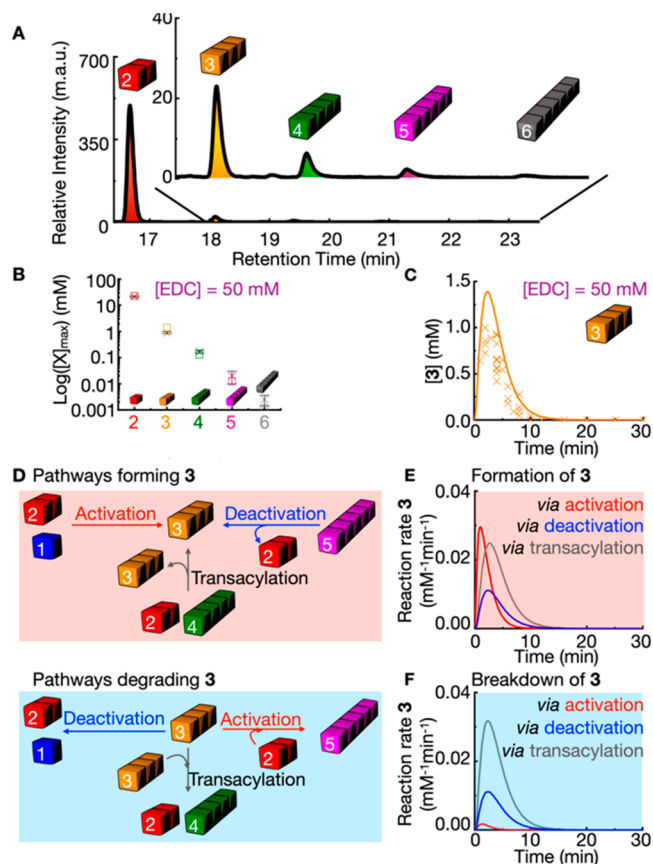


Figure 2. Response of the dynamic combinatorial library to a batch of fuel. (A) HPLC chromatogram of the transient dynamic combinatorial library made from **1**, when fueling with 50 mM EDC after 4 min. (B) Maximum concentration of the library compounds **2**–**6**, plotted on a logarithmic scale when fueling with 50 mM EDC (crosses). The data is an average of the maximum yields obtained in the reaction cycle. The kinetic model was used to fit the maximum yields (squares). (C) HPLC (markers, monitored at 290 nm) data of **3** when **1** was fueled with 50 mM EDC. The kinetic model was used to fit the experimental data (lines). (D) Schematic representation of example reactions for the build-up and breakdown of **3** by activation, deactivation, and transacylation. (E, F) Reaction rates for the formation and breakdown of **3** via activation, deactivation, or transacylation.

the rate constant of the reaction of **1** with EDC, yielding the *O*-acylisourea (k_1). We assumed that this activation rate constant is similar for all oligomer species. We then fitted the evolution of the *N*-acylisourea **1*** concentration to obtain the rate constants of its formation (k_3). Because the *O*-acylisourea was never observed, we ensured that **1** or the oligomers rapidly reacted toward the anhydride by choosing a high-rate constant attack of the *O*-acylisourea by **1** or the oligomers (k_2). We used the evolution of the anhydrides to fit k_4 and k_5 , which describe the anhydride hydrolysis and the transacylation reaction rate constants (Table S6). We considered that transacylation is faster than hydrolysis in the presence of pyridine.^{24,34,35} The fitted rate constant ensured that the kinetic model accurately predicted the decay of the concentration of EDC and the emergence of *N*-acylisourea **1*** (Figure S4A and G). It also captured the exponential decay of the maximum concentration of each oligomer as a function of oligomer length (Figure 2B). It is noteworthy that the model predicted the evolution

accurately for various sizes of EDC batches (Figures S4 and S5).

The kinetic model allows for extracting the individual reaction rates that dominate the evolution of the oligomers. For example, when we analyze the evolution of oligomer 3, we find three possible pathways to its formation (Figure 2D), i.e., the fuel-driven activation (e.g., 1 + 2 yields 3), the transacylation (e.g., 4 + 2 yields 3 + 3), or the deactivation of longer oligomers (e.g., 4 yields 3 + 1). Similarly, we find three possible pathways for the breakdown of oligomer 3, i.e., its spontaneous hydrolysis (deactivation), its transacylation (scrambling), or its activation into a longer oligomer (Figure 2D). In the first few minutes, the fuel-driven activation governs the formation of 3. However, we were surprised to find that, within minutes, the formation of 3 is dominated by the scrambling of other oligomers, e.g., the transacylation of two dimers 2 resulting in a 3 and a monomer 1 (Figure 2E). Even more surprising was that the breakdown kinetics of 3 is always dominated by the kinetics of transacylation as opposed to the deactivation via hydrolysis (Figure 2F). Specifically, the reaction that leads to most of the loss of 3 is the transacylation of 3, with 1 resulting in two molecules of 2. This loss via transacylation can be explained by the high concentrations of 1. Taken together, our kinetic model can capture the kinetics of the reaction cycle and reveals that the scrambling via transacylation plays an important role in the dynamics of our nonequilibrium system's chemistry (Figure 2D). Even though the activation and deactivation kinetics are dictated by nonequilibrium chemical reactions, the transacylation, which dominates the dynamics of the library, is an equilibrium reaction.

Next, we tested the response of the system to larger batch sizes of fuel, i.e., 75 and 100 mM. We were surprised to find that the maximum concentrations of the anhydrides did not decay exponentially with oligomer length as observed before (Figure 3A). While 2 had by far the highest maximum concentration, the maximum concentrations of oligomers 3, 4, 5, and 6 were similar at ~ 2.5 mM and much higher compared to the experiment with 50 mM fuel. The difference in the kinetics of the chemical reaction cycle was likely due to the oligomer's ability to self-assemble because the samples immediately turned turbid after the addition of the larger batches of fuel (Figure 3B). Moreover, the turbidity was a transient phenomenon, i.e., it decayed over 130 min, at which point the original transparency was restored. We imaged the rapid increase and subsequent decay of turbidity by time-lapse photography and measured the gray value of the samples with different batch sizes of EDC (Figure S6A and B). Fluorescence microscopy with the hydrophobic dye Nile red showed that micron-sized light-scattering particles were responsible for the increased turbidity (Figure 3C). Furthermore, cryogenic transmission electron microscopy (cryo-TEM) revealed a fibrillar substructure in the irregular micron-sized assemblies (Figure 3D). We measured the sample scattering rate by dynamic light scattering (DLS), which is a more sensitive measure of the presence of assemblies compared to the turbidity assays. The addition of 75 or 100 mM fuel drastically increased the scattering rate of our samples, whereas the addition of 50 mM or less did not, further corroborating that >50 mM fuel was needed to induce the formation of transient assemblies (Figure S7).

Ten minutes after the addition of fuel, we centrifuged the reaction solution and measured the concentration of the

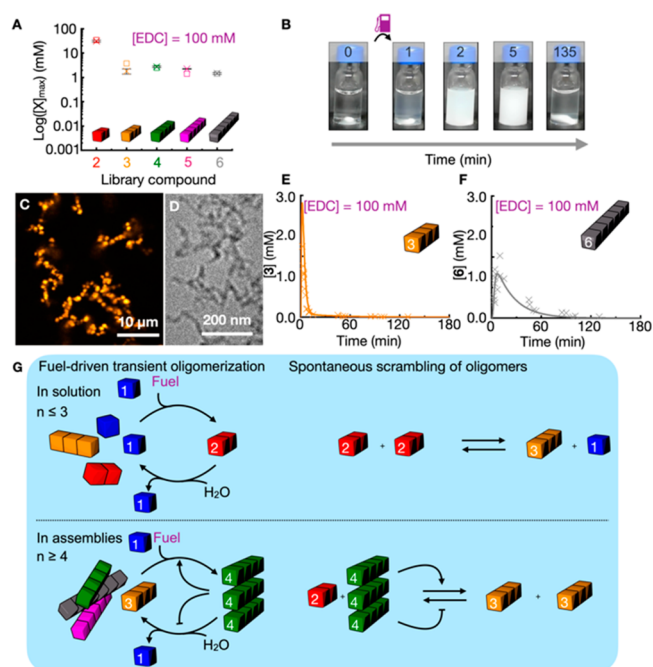


Figure 3. Response of the dynamic combinatorial library to a large batch of fuel. (A) Maximum concentrations of the library compounds 2–6, plotted on a logarithmic scale when fueling with 100 mM EDC (crosses). The data is an average of the maximum yields obtained in the reaction cycle. The kinetic model was used to fit the maximum yields (squares). (B) Photographs of 1 at different time points. (C) Micrograph of 1 and 25 μ M Nile red, fueled with 75 mM EDC after 5 min. (D) Cryo-TEM micrograph of 1 fueled with 75 mM EDC after 2 min. (E, F) HPLC data (markers, monitored at 290 nm) of 3 and 6, respectively, when 1 was fueled with 100 mM EDC. The kinetic model was used to fit the experimental data (lines). (G) Schematic representation of the feedback of assemblies on the deoligomerization reactions and scrambling reactions of the transient dynamic combinatorial library. Only oligomer 4 is shown in the scheme to save space.

oligomers in the supernatant and pellet. We found that the pellet contained mostly oligomers 4–6 (95 mol %) and only minor fractions of 2 and 3 (5.0 mol %) (Figure S6C and D). In contrast, the supernatant contained only 0.1 mM 4 but no 5 or 6. We conclude that library members 4–6 can assemble when a larger amount of fuel is added and that assembly can change the reaction kinetics, resulting in increasing yields of 4–6. Because of the ill-defined morphology of the assemblies and the huge polydispersity, we assume that all these library members randomly coassemble as opposed to self-sorting into individual assemblies.

We analyzed the evolution of the concentration of fuel and anhydrides 2–6 when assemblies were present (Figures 3E, S8, and S9). When 100 mM EDC was added, the fuel was entirely consumed within 16 min (Figure S9A). The concentrations of anhydrides 2–6 initially rose and then collapsed (Figures 3E and F and S9B–D). However, we observed a large difference in the deactivation kinetics of the oligomers that assembled (4–6) compared to those that did not (2 and 3, Figure 3E and F). For 100 mM EDC, we found that 2 and 3 peaked in the first few minutes and then decayed with first-order kinetics (Figures 3E and S10B). Moreover, at the time where the most fuel was consumed, these anhydrides had also mostly decayed. Surprisingly, 4, 5, and 6 peaked at ~ 9 min, which is close to the point where almost all fuel was depleted. Moreover,

beyond their peaks, their concentrations decayed much slower as compared to 2 and 3 (Figures 3F and S9C and D). It is noteworthy that the concentration of an unwanted side product, i.e., the *N*-acylisourea 1* of monomer 1, was <6 mM after the cycle was completed (Figure S9E).

From the combined results, we can conclude that, due to their ability to assemble, oligomers 4–6 are less reactive, likely because they are shielded from water and less mobile in their assemblies. These changes in the anhydride's microenvironment change their hydrolysis and transacylation rate constants. We adjusted our kinetic model in order to capture the much slower decays of 4, 5, and 6 due to their ability to assemble. In brief, we decreased the rate constants of deactivation and transacylation (k_4 and k_5) of those compounds until a good fit of the decay profile to the HPLC data was obtained for all oligomers (Figures 3E and F and S9, Table S6). Although the decay profiles of 4–6 were captured by the decreased rate constants of hydrolysis and transacylation, the yields of 3 and 4 remained overestimated, whereas the yields of 5 and 6 were underestimated. Therefore, we increased the rate constant of activation (k_1) for oligomers 4 and 5 and obtained good fits. Such an increase in the rate constant due to self-assembly could be explained by a surface catalysis mechanism.

To further confirm the role of self-assembly in these libraries, we carried out a seeding experiment. We first created a solution with assemblies, spun down the assemblies, removed the supernatant, and resuspended them in the buffer. A small fraction of this solution was added to an experiment of 300 mM 1 fueled with 30 mM EDC. Without the seed in that experiment, no 5 or 6 was observed (Figure S10). With the seed, the maximum concentration of 5 was ~0.3 mM. Moreover, the concentration of 5 was almost double compared to the amount of the added seed, demonstrating that new 5 was made. Only when the feedback mechanisms were taken into account in our kinetic model could the evolution of 5 be well-predicted in the described seeding experiment (Figure S11).

From the combined data sets, we can make the following observations. Our chemically fueled, dynamic combinatorial library is governed by in-equilibrium and out-of-equilibrium reaction kinetics, as exemplarily illustrated for part of the library in Figure 3G. The fuel-driven activation reaction and the spontaneous hydrolysis are of nonequilibrium nature. In contrast, the transacylation reaction is an equilibrium reaction. All these reactions are happening simultaneously at comparable rates, which makes the interpretation of the data nearly impossible without the use of a kinetic model. Our kinetic model shows that the reaction kinetics of the individual library members are largely dominated by the in-equilibrium transacylation, i.e., transacylation recombines the library components while maintaining the average oligomer length. However, the global and transient shift toward longer oligomer members is driven by the fuel-consuming activation reactions (Figure 3G).

Our study has focused on the transient formation of a dynamic combinatorial library in response to a batch of chemical energy, which allowed us to write a kinetic model. To mimic better the complexity of chemical reaction networks in biology, we designed experiments that are regulated by the continuous transduction of energy. A vial was continuously fueled, via a microsyringe pump, with 100 mM h⁻¹ EDC (Figure 4A). It is noteworthy that the reactor was continuously stirred and had no outlet ports, i.e., we used a continuously

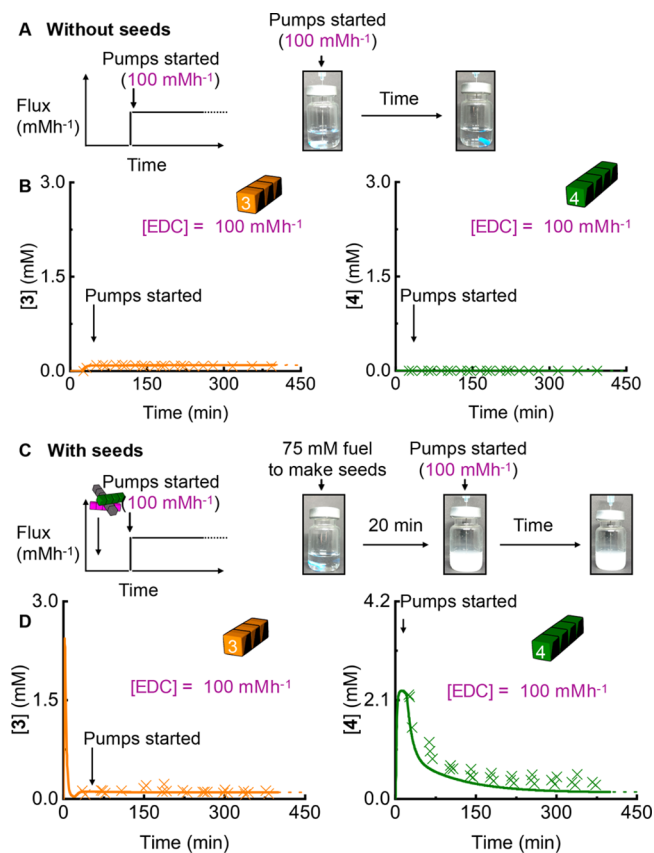


Figure 4. Response of the dynamic combinatorial library to continuous transduction of fuel. (A, C) Schematic experimental setup of continuous fueled experiments in the absence (A) and presence (C) of a seed. (B, D) HPLC (markers, monitored at 290 nm) data of 3 and 4 when 1 was continuously fueled with 100 mM EDC/h in either the absence (B) or presence of a seed (D). The kinetic model was used to fit the experimental data (lines).

stirred batch reactor. By the naked eye, we found that the sample remained clear. HPLC analysis revealed that only oligomers 2 and 3 were formed in measurable amounts and were stable in a steady state over the course of the experiment (Figure 4B). Our kinetic model could accurately predict the evolution well (Figures 4B and S12).

Given the ability of our assemblies to exert negative feedback on their deactivation reactions, we were curious to see whether their presence could affect steady states; e.g., could the presence of a higher number of oligomers, as a seed, increase their likelihood of survival (Figure 4C)? Thus, we formed the seeds by the addition of a batch of 75 mM fuel to the solution of monomer 1. We then waited 20 min to ensure that all EDC had converted to EDU and the major components in the vial were 4, 5, and 6, i.e., a seed of longer oligomers (Figure 4C). Then, we started to continuously fuel the system with 100 mM h⁻¹ EDC (Figure 4C). We found that the concentrations of longer oligomers 4–6 decreased until a steady-state level was reached. That steady state was much higher compared to the experiment without seeds in which 4, 5, and 6 were not detected (Figures 4D and S13). Moreover, when we performed a similar experiment with 100 mM fuel as a spike, we observed very similar behavior (Figures S13 and S14). It is noteworthy that our kinetic model predicted the experimentally observed evolution of the concentration profiles of all oligomers. Taken together, the presence of the assembly as a seed initiates the

feedback mechanisms, which helps the survival of longer oligomers. Because of the feedback mechanisms, the outcome of the experiment on whether assemblies are present depends on the history of the sample. Such behavior is ubiquitous in biology and is used for decision-making, but synthetic counterparts are rare.^{11,36}

CONCLUSION

Previous work on chemically fueled systems has mainly focused on how chemical reactions regulate the self-assembly behavior of one molecule. Because of the molecular design of the precursor in this work, the product of one cycle is the precursor for the next. This dynamic combinatorial library approach opens the door to emergent mechanisms in which sequences can be selectively up- or down- concentrated. In the system we described, monomers can be oligomerized, oligomers can be deoligomerized, and oligomers can transacylate. Surprisingly, we found that the dynamics of the individual components of the library were dominated by transacylation, which is an equilibrium reaction. In contrast, the dynamics of the entire library were dictated by fuel-driven activation, which is a nonequilibrium reaction. Finally, we find that self-assembly can play a large role in affecting the kinetics of the reactions via feedback mechanisms. The interplay of the simultaneously operating reactions and feedback mechanisms can result in hysteresis effects in which the outcome of the competition for fuel depends on events that occurred in the past, i.e., via the presence of seeds. In future work, we envision diversifying the library by modifying building blocks with catalytically active motifs. In such mixtures, we expect coassembly, self-sorting, and perhaps even hybridization of the oligomers to result in feedback mechanisms by which information-containing sequences can be spontaneously selected from a pool of simple building blocks when supplied with chemical energy.

ASSOCIATED CONTENT

Supporting Information

The Supporting Information is available free of charge at <https://pubs.acs.org/doi/10.1021/jacs.1c01616>.

Kinetic model (ZIP)

Materials and methods description; additional data on the transacylation; additional data on the characterization of precursor and product (ESI-MS, HPLC); additional kinetic data; description of the used kinetic model and the observed and fitted rate constants; and time-lapse photographs (PDF)

AUTHOR INFORMATION

Corresponding Author

Job Boekhoven – Department of Chemistry, Technical University of Munich, 85748 Garching, Germany; Institute for Advanced Study, Technical University of Munich, 85748 Garching, Germany; orcid.org/0000-0002-9126-2430; Email: job.boekhoven@tum.de

Authors

Christine M. E. Kriebisch – Department of Chemistry, Technical University of Munich, 85748 Garching, Germany
Alexander M. Bergmann – Department of Chemistry, Technical University of Munich, 85748 Garching, Germany

Complete contact information is available at:

<https://pubs.acs.org/10.1021/jacs.1c01616>

Notes

The authors declare no competing financial interest.

ACKNOWLEDGMENTS

This research was funded by the Volkswagen Foundation via the Life? program and was conducted within the Max Planck School Matter to Life supported by the German Federal Ministry of Education and Research (BMBF) in collaboration with the Max Planck Society. J.B. is grateful for support by the European Research Council (ERC starting Grant 852187) and the Deutsche Forschungsgemeinschaft (DFG, German Research Foundation) – Project-ID 364653263 – TRR 235. Cryo-TEM measurements were performed using infrastructure contributed by the Dietz Lab and the TUM EM Core Facility. We acknowledge the technical support provided by Fabian Kohler.

ABBREVIATIONS

Cryo-TEM, cryogenic transmission electron microscopy; EDC, 1-ethyl-3-(3-(dimethylamino)propyl)carbodiimide; ESI-MS, electrospray ionization–mass spectrometry; HPLC, high-performance liquid chromatography; MES, 2-(*N*-morpholino)-ethanesulfonic acid

REFERENCES

- (1) Li, J.; Nowak, P.; Otto, S. Dynamic Combinatorial Libraries: From Exploring Molecular Recognition to Systems Chemistry. *J. Am. Chem. Soc.* **2013**, *135* (25), 9222–9239.
- (2) Hunt, R. A. R.; Otto, S. Dynamic combinatorial libraries: new opportunities in systems chemistry. *Chem. Commun.* **2011**, *47* (3), 847–858.
- (3) Ludlow, R. F.; Otto, S. Systems chemistry. *Chem. Soc. Rev.* **2008**, *37* (1), 101–108.
- (4) Von Bertalanffy, L. The Theory of Open Systems in Physics and Biology. *Science* **1950**, *111* (2872), 23–29.
- (5) Pross, A. Stability in chemistry and biology: Life as a kinetic state of matter. *Pure Appl. Chem.* **2005**, *77* (11), 1905–1921.
- (6) Pross, A.; Pascal, R. How and why kinetics, thermodynamics, and chemistry induce the logic of biological evolution. *Beilstein J. Org. Chem.* **2017**, *13*, 665–674.
- (7) Lehman, N. A recombination-based model for the origin and early evolution of genetic information. *Chem. Biodiversity* **2008**, *5* (9), 1707–17.
- (8) Mutschler, H.; Taylor, A. I.; Porebski, B. T.; Lightowlers, A.; Houlihan, G.; Abramov, M.; Herdewijn, P.; Holliger, P. Random-sequence genetic oligomer pools display an innate potential for ligation and recombination. *eLife* **2018**, *7*, e43022.
- (9) Blokhuis, A.; Lacoste, D. Length and sequence relaxation of copolymers under recombination reactions. *J. Chem. Phys.* **2017**, *147* (9), 094905.
- (10) Smail, B. A.; Clifton, B. E.; Mizuuchi, R.; Lehman, N. Spontaneous advent of genetic diversity in RNA populations through multiple recombination mechanisms. *RNA* **2019**, *25* (4), 453–464.
- (11) Semenov, S. N.; Kraft, L. J.; Ainla, A.; Zhao, M.; Baghbanzadeh, M.; Campbell, V. E.; Kang, K.; Fox, J. M.; Whitesides, G. M. Autocatalytic, bistable, oscillatory networks of biologically relevant organic reactions. *Nature* **2016**, *537* (7622), 656–660.
- (12) Cafferty, B. J.; Wong, A. S. Y.; Semenov, S. N.; Belding, L.; Gmür, S.; Huck, W. T. S.; Whitesides, G. M. Robustness, Entrainment, and Hybridization in Dissipative Molecular Networks, and the Origin of Life. *J. Am. Chem. Soc.* **2019**, *141* (20), 8289–8295.
- (13) Maguire, O. R.; Wong, A. S. Y.; Baltussen, M. G.; van Duppen, P.; Pogodaev, A. A.; Huck, W. T. S. Dynamic Environments as a Tool

to Preserve Desired Output in a Chemical Reaction Network. *Chem. - Eur. J.* **2020**, *26* (7), 1676–1682.

(14) Tena-Solsona, M.; Rieß, B.; Grötsch, R. K.; Löhner, F. C.; Wanzke, C.; Käsdorf, B.; Bausch, A. R.; Müller-Buschbaum, P.; Lieleg, O.; Boekhoven, J. Non-equilibrium dissipative supramolecular materials with a tunable lifetime. *Nat. Commun.* **2017**, *8*, 15895.

(15) van Rossum, S. A. P.; Tena-Solsona, M.; van Esch, J. H.; Eelkema, R.; Boekhoven, J. Dissipative out-of-equilibrium assembly of man-made supramolecular materials. *Chem. Soc. Rev.* **2017**, *46* (18), 5519–5535.

(16) Boekhoven, J.; Hendriksen, W. E.; Koper, G. J. M.; Eelkema, R.; van Esch, J. H. Transient assembly of active materials fueled by a chemical reaction. *Science* **2015**, *349* (6252), 1075.

(17) Pappas, C. G.; Mutasa, T.; Frederix, P. W. J. M.; Fleming, S.; Bai, S.; Debnath, S.; Kelly, S. M.; Gachagan, A.; Ulijn, R. V. Transient supramolecular reconfiguration of peptide nanostructures using ultrasound. *Mater. Horiz.* **2015**, *2* (2), 198–202.

(18) Heuser, T.; Weyandt, E.; Walther, A. Biocatalytic Feedback-Driven Temporal Programming of Self-Regulating Peptide Hydrogels. *Angew. Chem., Int. Ed.* **2015**, *54* (45), 13258–13262.

(19) Sorrenti, A.; Leira-Iglesias, J.; Sato, A.; Hermans, T. M. Non-equilibrium steady states in supramolecular polymerization. *Nat. Commun.* **2017**, *8* (1), 15899.

(20) Maiti, S.; Fortunati, I.; Ferrante, C.; Scrimin, P.; Prins, L. J. Dissipative self-assembly of vesicular nanoreactors. *Nat. Chem.* **2016**, *8* (7), 725–31.

(21) Del Grosso, E.; Prins, L. J.; Ricci, F. Transient DNA-Based Nanostructures Controlled by Redox Inputs. *Angew. Chem., Int. Ed.* **2020**, *59* (32), 13238–13245.

(22) Panja, S.; Patterson, C.; Adams, D. J. Temporally-Programmed Transient Supramolecular Gels. *Macromol. Rapid Commun.* **2019**, *40* (15), 1900251.

(23) Bal, S.; Das, K.; Ahmed, S.; Das, D. Chemically Fueled Dissipative Self-Assembly that Exploits Cooperative Catalysis. *Angew. Chem., Int. Ed.* **2019**, *58* (1), 244–247.

(24) Hossain, M. M.; Atkinson, J. L.; Hartley, C. S. Dissipative Assembly of Macrocycles Comprising Multiple Transient Bonds. *Angew. Chem., Int. Ed.* **2020**, *59* (33), 13807–13813.

(25) Kriebisch, B. A. K.; Jussupow, A.; Bergmann, A. M.; Kohler, F.; Dietz, H.; Kaila, V. R. I.; Boekhoven, J. Reciprocal Coupling in Chemically Fueled Assembly: A Reaction Cycle Regulates Self-Assembly and Vice Versa. *J. Am. Chem. Soc.* **2020**, *142* (49), 20837–20844.

(26) Späth, F.; Donau, C.; Bergmann, A. M.; Kränzlein, M.; Synatschke, C. V.; Rieger, B.; Boekhoven, J. Molecular Design of Chemically Fueled Peptide–Polyelectrolyte Coacervate-Based Assemblies. *J. Am. Chem. Soc.* **2021**, *143* (12), 4782–4789.

(27) Kariyawasam, L. S.; Hossain, M. M.; Hartley, C. S. The Transient Covalent Bond in Abiotic Nonequilibrium Systems. *Angew. Chem., Int. Ed.* **2021**, *60*, 2–16.

(28) Singh, N.; Formon, G. J. M.; De Piccoli, S.; Hermans, T. M. Devising Synthetic Reaction Cycles for Dissipative Nonequilibrium Self-Assembly. *Adv. Mater. (Weinheim, Ger.)* **2020**, *32* (20), 1906834.

(29) Rieß, B.; Grötsch, R. K.; Boekhoven, J. The Design of Dissipative Molecular Assemblies Driven by Chemical Reaction Cycles. *Chem.* **2020**, *6* (3), 552–578.

(30) Tena-Solsona, M.; Wanzke, C.; Riess, B.; Bausch, A. R.; Boekhoven, J. Self-selection of dissipative assemblies driven by primitive chemical reaction networks. *Nat. Commun.* **2018**, *9* (1), 2044.

(31) Yang, S.; Schaeffer, G.; Mattia, E.; Markovitch, O.; Liu, K.; Hussain, A. S.; Ottelé, J.; Sood, A.; Otto, S. Chemical Fueling Enables Molecular Complexification of Self-Replicators. *Angew. Chem., Int. Ed.* **2021**, DOI: 10.1002/anie.202016196 (accessed 3/25/2021).

(32) Bucher, J. E.; Slade, W. C. The Anhydrides of Isophthalic and Terephthalic Acids. *J. Am. Chem. Soc.* **1909**, *31* (12), 1319–1321.

(33) Domb, A. J.; Langer, R. Polyanhydrides. I. Preparation of high molecular weight polyanhydrides. *J. Polym. Sci., Part A: Polym. Chem.* **1987**, *25* (12), 3373–3386.

(34) Bunton, C. A.; Fuller, N. A.; Perry, S. G.; Shiner, V. J. The pyridine catalysed hydrolysis of carboxylic anhydrides. *Tetrahedron Lett.* **1961**, *2* (14), 458–460.

(35) Fersht, A. R.; Jencks, W. P. Acetylpyridinium ion intermediate in pyridine-catalyzed hydrolysis and acyl transfer reactions of acetic anhydride. Observation, kinetics, structure-reactivity correlations, and effects of concentrated salt solutions. *J. Am. Chem. Soc.* **1970**, *92* (18), 5432–5442.

(36) Maity, I.; Wagner, N.; Mukherjee, R.; Dev, D.; Peacock-Lopez, E.; Cohen-Luria, R.; Ashkenasy, G. A chemically fueled non-enzymatic bistable network. *Nat. Commun.* **2019**, *10* (1), 4636.